OPEN ACCESS
Freely Available Online

JOURNAL OF SYSTEMS BIOLOGY
ISSN NO: COMING SOON

Research Article

DOI : COMING SOON

Retinal and Cortical Contributions to Excessive V1 Neuron Firing Rate Variability in Schizophrenia: A Computational Modeling Analysis

Steven M. Silverstein[1,2,3,4,*], Hristiyan Kourtev[2]

[1]Rutgers-Princeton Center for Computational Cognitive Neuropsychiatry

[2]Rutgers Center for Cognitive Science

[3]Departments of Psychiatry and Ophthalmology

[4]University Behavioral Health Care

Abstract

Excessive variability in behavioral performance and neuronal activation is a common finding in studies of schizophrenia. Recent evidence suggests that this may be due to an imbalance in the ratio of excitation to inhibition in brain function, or *E/I imbalance*. We used computational modeling of visual system activity to determine whether different potential causes of E/I imbalance would generate effects resembling those reported in schizophrenia. Three major findings emerged. First, reductions in retinal and lateral geniculate nucleus signaling initially led to increases in firing rate variability within the context of reduced V1 activation; however, with prolonged adaptation to weakened sensory signaling, compensatory hyper-activation in V1 neurons occurred, but variability was no longer increased. Second, direct increases in V1 excitation, or decreases in inhibition, led to the highest levels of initial activation but not variability; however, with prolonged inhibitory adaptation to increased excitation, overall activity was no longer elevated, but an increase in firing rate variability was observed. Third, the greatest fluctuation in firing rate variability, in response to the same stimulus across increasing contrast levels, was observed with reductions in sensory signaling, but only immediately after model perturbations; with prolonged adaption, the largest fluctuations were associated with increased excitation or reduced inhibition within V1. Implication of these findings are that schizophrenia-related increases in neuronal response variability may arise from at least two sources: 1) weakened sensory signaling and its associated low signal-to-noise ratio; and 2) compensatory but incomplete inhibitory responses to continuous increases in cortical excitation.

Corresponding author: Steven M. Silverstein, Rutgers University Behavioral Health Care, 671 Hoes Lane West, Room D351, Piscataway, NJ 08854, ORCID ID: 0000-0002-0699-0960. Email: steven.silverstein@rutgers.edu.

Keywords: V1, Schizophrenia, Excitation-Inhibition balance, Computational Psychiatry, Vision, Variability, Retina, LGN.

Received: Jan 05, 2019 **Accepted:** Jan 23, 2019 **Published:** Jan 30, 2019

Editor: Sutopa Dwivedi, University of Pennsylvania, United States.

Introduction

The visual system is an excellent system within which to characterize between-group differences in neural computations [1]. This is because computational theories of vision are well-established, the neural basis of early vision is well-understood, vision is the most studied area of neuroscience, and many of the neural computations involved in vision are found throughout the cortex but can arguably be isolated more easily when studying the occipital lobe [1-5].

People with schizophrenia demonstrate a wide range of visual processing impairments, ranging from altered retinal activity to disturbances in high-level visual cognition [3]. Nearly all past studies of these issues have focused on schizophrenia-control group differences in mean levels of behavioral performance or neural activation, with very little focused exploration of differences in indicators of systematic deviation from normal patterns of performance (e.g., range, standard deviation, skew, kurtosis, coefficient of variation). However, parameters related to variation can provide unique information about brain function [6-12]. To date, studies of schizophrenia that have focused on within-task variability in behavioral or electrophysiological responses [e.g., [12, 13]] have explored consistency in those responses to identical stimuli, rather than deviation from an expected degree of variation across trials wherein a single parameter is systematically manipulated. Because the degree to which stimulus intensity increases are associated with systematic neural activation increases can be taken as a measure of the precision with which stimulus differences are represented at the neural and perceptual levels, deviations from this rate can be expected to have perceptual consequences. Therefore, our focus was on the degree to which deviation from normal levels of variability in firing rates, across a sequence of stimuli that increased in intensity along a single dimension, but also across V1 neurons in response to a single stimulus, would emerge in schizophrenia-relevant models. In the models we tested, we focused on parameters and values that were associated, in our prior computational modeling work [14], with good fits to previously published data on: 1) both reduced contrast sensitivity (CS) and broadened orientation (OR) tuning in chronic schizophrenia; and 2) excessive CS in first episode schizophrenia (FES) [3, 15, 16]. This was done to determine whether parameter manipulations associated with well-known visual processing impairments in schizophrenia would also be associated with an abnormal degree of deviance from expected activation values. Of note, all parameter manipulations used involved an imbalance in the ratio of cortical excitation and inhibition, or *E/I imbalance*, which recently has been a focus in schizophrenia research, and is thought to be a cause of excessive within-task variability in people with the disorder [17-19]. With a focus on the coefficient of variation as the primary index of activation deviance, our results show that deviation from the normal range of firing rates is: 1) not a necessary consequence of either increases or decreases in overall mean activation; 2) a result of long-term adaptation to increased excitation; and 3) an initial, but not long-term result of weakened sensory input to visual cortex. These data thus highlight the importance of viewing specific perceptual changes in schizophrenia within an illness-development perspective.

Methods

Modeling Environment

All models were run using the Topographica simulator [20-22], which is freely available at https://github.com/ioam/topographica, with documentation at www.topographica.org. Topographica was developed for modeling the development of cortical maps, and has been typically used for computational modeling of aspects of low- and mid-level vision (e.g., orientation preference maps, orientation tuning, contrast sensitivity, aftereffects).

Baseline Model Characteristics

For this project, we used as our baseline the GCAL (gain control, adaptation, laterally connected) model [[23], further described in [20-22]]. GCAL incorporates features that are biologically realistic, including: 1) gain control at the lateral geniculate nucleus (LGN) level; 2) homeostatic adaptation of V1 responses based on a weighted sum of all inputs and limited by a logistic (sigmoid) nonlinearity; and 3) weights on excitatory and inhibitory lateral connections within V1, and on afferent connections to V1. These weights begin as isotropic (radially uniform), but subsequently modify in a self-organizing fashion upon repeated presentations of visual input and other forms of

neural activity (e.g., lateral interactions) according to Hebbian (unsupervised activity-dependent) learning, with divisive normalization. Other characteristics of the GCAL model include: the assumption of single-compartment firing-rate neurons at the retinal ganglion cell, LGN, and V1 levels; hard-wired subcortical pathways to V1, including the main types of LGN neurons (e.g., On center-Off surround; Off center-On surround); roughly retinotopic projections from the retina to the LGN sheets to the V1 sheet; and separate parameters for excitatory and inhibitory activity (see Figure 1). GCAL has successfully modeled a wide range of phenomena expressed in a healthy V1, such as development of contrast-invariant orientation tuning and direction selectivity, development of ocular dominance, aftereffects, and surround suppression. Such modeling results show that these effects can be explained by a small number of canonical mechanisms [21, 24-27]. These demonstrations also indicate that through visual experience, the statistical regularities of the environment are learned and encoded via the competitive processes inherent to Hebbian learning, and that these processes are constrained by gain control and homeostatic mechanisms to prevent runaway neural excitation and excessive plasticity in frequently activated circuits.

The basic GCAL model has four levels or sheets, each of which is implemented as a two-dimensional array of firing-rate neurons: a retina (24 x 24 density), LGN On and Off channel sheets (24 x 24 density), and a V1 sheet (48 x 48 density) (see Figure 1). Here, 'density' represents the number of simulated units (neurons) per unit area of the indicated sheet, corresponding to a square portion of the simulated visual field. The retina and LGN sheets thus have ¼ the number of units per visual area as does the V1 sheet. As illustrated in Figure 1, these four sheets are interconnected via sets of projections, or 'connection fields,' whose synaptic weights on the next sheet level are modifiable by

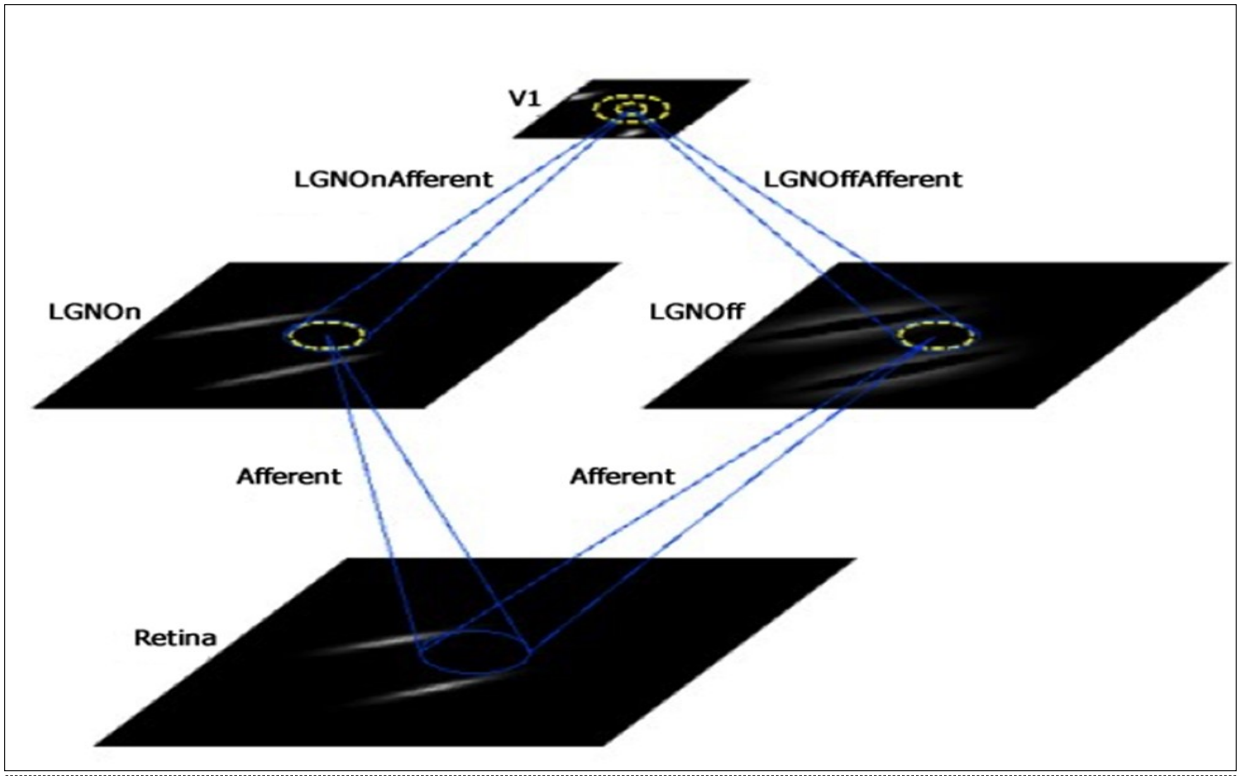

Figure 1. Depiction of the sheets and connections in the GCAL class of models used in this study. Sheets include Retina, LGN On and LGN Off, and V1. Projections include afferent input to each of the LGN sheets, and afferent input to V1 from each of the LGN sheets, as well as lateral excitatory feedback within V1 (inner yellow circle) and a wider range of lateral inhibitory feedback within V1 (outer yellow circle). Examples of the training stimuli used in each model (i.e., pairs of orientated Gaussians) can be seen in the Retina sheet, with corresponding transformations in the LGN and V1 sheets.

Hebbian learning, and by changes in learning rates. Note that in GCAL models, the retina sheet is equivalent to the photoreceptor layer of the retina only. The model LGN sheet activity is an abstraction that represents all levels between the photoreceptors and the superficial layers of V1 that combine and transform the photoreceptor signals, including the retinal bipolar and ganglion cell layers and the LGN itself.

In all models presented here, activity was simulated in a series of time steps, with each corresponding to approximately 12.5 milliseconds in real time. At step 1 (t=0), the image reaches the retina, at step 2 the LGN On and Off sheets calculate their responses, at step 3 the output of the LGN On and Off sheets reaches the V1 sheet, and from steps 4 to 20 the activity within the V1 sheet propagates and settles through lateral inhibitory and excitatory connections. At the next step, the next stimulus is presented to the retina, and this repetition of sets of 20 steps continues for the number of iterations (i.e., stimulus presentation trials) chosen by the user.

Model Parameter Manipulations

For this project, we, for the most part, limited manipulations to those that provided the best fit to published data in our prior study [14], to determine if the same manipulations that led to CS and OR tuning changes could also account for increased neural variability. The specific manipulations we examined, and a rationale for their use, are described below.

Changes in Input Strength: Several lines of evidence indicate that afferent input to the LGN is reduced in schizophrenia. First, schizophrenia is associated with reduced retinal photoreceptor and bipolar cell signaling as indicated by smaller flash electroretinogram (ERG) waveform amplitudes [28-33], and this change is more pronounced in patients at the outset of treatment for an acute psychotic episode than it is after several weeks of treatment. Preliminary data also indicate reduced activity in retinal ganglion cells [29], whose axons form the optic nerve and synapse directly onto the LGN. Second, reduced retinal signaling could be expected to reduce the strength of LGN output and therefore the strength of signals reaching V1, and indeed, reduced amplitudes of visual evoked potentials (VEPs) have been repeatedly observed in schizophrenia, with evidence that the problem is more pronounced in unmedicated patients [reviewed in [34-36]]. For this study, we examined V1 neural variability as a function of a 15% reduction in both retinal and LGN efferent signals. This manipulation led to compensatory hyperactivation in model V1 neurons in our prior modeling study [14], and provided a good fit to the increased CS seen in unmedicated first episode schizophrenia patients [reviewed in [3]].

Changes in Excitation and Inhibition

Reduced lateral inhibition within V1. The strength of inhibition within V1 was reduced based on findings of reduced GABA concentration in the visual cortex of people with schizophrenia [37-39], as well as on findings of broadened OR tuning in cat after administration of the selective $GABA_A$ antagonist gabazine [40]. For the purposes of this study, a 10% reduction in V1 lateral inhibition strength was explored, as this change, in combination with an increase in the V1 afferent learning rate (see below, Changes in Plasticity) provided the best fit to published data on reduced CS and broadened OR tuning in chronic schizophrenia [14].

Increased lateral excitation within V1. Two sources of evidence suggest elevated local excitatory activity within V1. One is the similarity between hyper-glutamatergic effects of ketamine administration in healthy volunteers and brain function in schizophrenia [41-43]. The second is evidence for elevated baseline gamma- and beta-band power and synchrony in people with schizophrenia [44-46], suggesting abnormal network formation. For the purposes of this study, a 10% increase in V1 lateral excitation strength was explored, to parallel the extent of changes in inhibition.

Changes in Plasticity

Increased afferent learning rate at LGN-to-V1 connections. This manipulation to the Hebbian learning rate was based on findings of reduced reliability in neuronal co-activation patterns in schizophrenia [47], and tighter coupling between thalamic and cortical sensory processing regions in schizophrenia compared to healthy controls [48]. This manipulation, in the form of a threefold increase in learning rate, was used only in combination with a 10% reduction in the V1 lateral inhibition rate, as this combination provided the best fit

to published data on reduced CS and broadened OR tuning in chronic schizophrenia in our prior study [14].

Model Function

We followed the model architecture and parameter settings from [23] except as specifically noted. Below, only the key algorithms related to activation, learning, and adaptation will be described, as these are most relevant to understanding the study's schizophrenia-related parameter changes and findings relating to CS and OR tuning. These algorithms are the same as those described in [14].

In GCAL, the activation value (i.e., firing rate) in each unit in the retina sheet is the brightness of that pixel in the training image. Training stimuli (i.e., those that the models were exposed to during their 20,000 developmental iterations; see below Model Training and Development Strategy) were pairs of elongated Gaussians (see Figure 1). The center coordinates of each Gaussian were chosen from a random distribution, and the patterns covered an area that was calculated as 1/3 larger than the V1 sheet lengthwise and heightwise. This ensured that all regions of the V1 sheet were equally likely to be stimulated during training.

For each unit at position j in the LGN On and Off sheets (O), activation at time $t+\delta t$ was calculated as:

$$\eta_{j,O}(t + \delta t) = f * \frac{\gamma_O \sum_{i \in F_{j,P}} \Psi_i(t)\,\omega_{ij}}{k + \gamma_S \sum_{i \in F_{j,S}} \eta_{i,O}(t)\,\omega_{ij,S}} \qquad \text{Eq 1}$$

Where γ_O = 14.0, set as a constant so that the overall strength of connections from the photoreceptor sheet to the LGN On and Off sheets will produce activations within the range of 0.0 to 1.0; γ_S is the strength of feedforward contrast gain control; Ψ_i is the activation of unit i in the two-dimensional array of neurons on the photoreceptor sheet from which LGN (On or Off) sheet unit j receives input (i.e., its afferent connection field $F_{j,P}$), and $\eta_{i,O}(t)$ is the activation in other units in the LGN (On or Off) sheet at the previous time step (received over the suppressive connection field $F_{j,S}$); f is a half-wave rectifying function that ensures that activation values of LGN On and Off sheet units are always positive; the constant k = .11 ensures that output is always significant even for weak inputs; ω_{ij} is the fixed connection weight between retinal sheet unit i and LGN sheet j defined as a standard difference of Gaussian kernels (to ensure that an On sheet unit is activated only when there is both high center activity and low surround activity, and that an Off sheet unit is activated only when there is both low center activity and high surround activity) ([23], see equation 3 for further details about derivation of these weight values); $\omega_{ij,S}$ and represents the spatial profile of lateral inhibition received from other units in the same LGN sheet: these weights have a fixed, circular Gaussian profile (see [23], equation 4 for further details), and they have a divisive effect on LGN sheet activity that functions to implement contrast gain control.

For each unit (j) in the V1 sheet, activity is calculated as a function of the local connection field on and around j. The connection field (F_{jp}) consists of both incoming projections (p) from another (e.g., LGN) sheet (s_p), and activity in the inhibitory and excitatory lateral connections to that unit. The total contribution (C_{jp}) to j from projection p from each projection type is a dot product of the input and the weights in each connection field, or:

$$C_{j,p}(t + \delta t) = \sum_{i \in F_{j,p}} \eta_{i,p}(t)\,\omega_{ij,p} \qquad \text{Eq 2}$$

Where is $\eta_{i,p}$ the *activation* in unit i reflecting all of the neurons in V1 of a single projection type with which unit j is connected, and $\omega_{ij,p}$ is the connection *weight* from unit i to unit j in V1 for each projection type. The contributions from each projection type are combined to calculate the activation of each neuron j in V1 at time t as follows:

$$\eta_{j,v}(t) = f * \sum_{p} \gamma_p C_{jp(t)} \qquad \text{Eq 3}$$

In the baseline GCAL model, the strength of each projection type was set as follows: γ_a (afferent) = 1.5, γ_E (excitatory) = 1.7, and γ_I (inhibitory) = -1.4. These values were shown to provide an appropriate balance between afferent and lateral influences, and between excitatory and inhibitory connections, and to lead to smooth and normally developing orientation and other topographic maps in the V1 sheet [23]. The variable f is a half-wave rectifying function to ensure positive activation values, and its threshold value (θ) varies as a function of the average activity of the unit, as part of implementing homeostasis (see below, next

two paragraphs).

From times t + 0.15 to t + 0.95 (i.e., steps 3 through 20 after each stimulus presentation), activity settles in V1, as noted above. At the end of this settling process, the level of activation in each V1 unit j is used to update the activation threshold point θ (see below) of each unit and to update the afferent and lateral inhibitory weights using the standard Hebbian learning algorithm (see below). V1 activity is then reset to 0.0 and a new stimulus is presented to the model.

The activation threshold θ determines how much a V1 unit will fire in response to an input. To determine the activation threshold for each V1 unit, a smoothed exponential average of its settled activity patterns is calculated:

$$\bar{\eta}_j(t) = (1-\beta)\eta_j(t) + \beta\bar{\eta}_j(t-1) \qquad \text{Eq 4}$$

where the parameter , β here set at 0.9999, determines the degree of smoothing in the calculation of the mean. The variable $\bar{\eta}_j$ is initially set to a target average for V1 unit activity, which is set to $\bar{\eta}_{jA}(0)$= μ = 0.024. The threshold value θ is then updated as follows:

$$\theta(t) = \theta(t-1) + \lambda(\bar{\eta}_j(t) - \mu) \qquad \text{Eq 5}$$

where λ is set at 0.01 and is the homeostatic learning rate, or the rate at which the average activity in each V1 unit is brought closer to the specified target value μ. If the mean activity level in a V1 unit begins to deviate from μ during model activity, the threshold θ is raised or lowered in order to bring the value back closer to μ.

As noted above, prior to any stimulus presentations to the model, connection weights from all projections to and within V1 ($\omega_{ij,p}$) are roughly isotropic (radially uniform), with the constraint that weights for each type of projection are operative within different circular radii [(to enable, for example, a more narrow zone of lateral excitation surrounded by a larger zone where inhibitory effects operate, consistent with known cortical function [49, 50]]. Radii for GCAL, for afferent, lateral excitatory, and lateral inhibitory connections respectively were set to: r_A=0.27, r_E=0.1, and r_I=0.23.

As stimuli are presented to the model, afferent connection weights from the LGN On and Off sheets are updated each time the V1 settling process is completed (i.e., every 20 steps, or once per iteration). The updating is based on a Hebbian learning rule, leading to the development of connection strengths that represent correlations between the LGN On and Off unit outputs and the postsynaptic V1 response. At each iteration, the weight adjustment is therefore dependent on three factors: presynaptic (LGN) activity (η_i), postsynaptic (V1) activity (η_j), and the Hebbian learning rate (α), with specific influences as follows:

$$\omega_{ij,p}(t) = \frac{\omega_{ij,p}(t-1) + \alpha\eta_j\eta_i}{\sum_k(\omega_{kj,p}(t-1) + \alpha\eta_j\eta_k)} \qquad \text{Eq 6}$$

where for each V1 unit j, α is the Hebbian learning rate for the afferent projection. Because unless Hebbian learning is constrained, it will lead to overly frequent changes in weight values and thus unstable network function [51], a constraint was added to impose divisive (postsynaptic) normalization on the V1 weight values. This well-understood mechanism [52, 53] was implemented via the denominator in the equation immediately above. For the baseline GCAL model, learning rates for afferent projections, lateral excitatory projections, and lateral inhibitory projections were set respectively to α_A=0.01, α_E=0.00, and α_I=0.03 [as in [23]]. As noted below, in several cases in this study modifications were made to these learning rates to explore the potential contributions of reduced stability within V1 on CS and OR tuning in schizophrenia.

Model Training and Development Strategy

For this study, we operationalized variability in three ways: 1) the spread of activation values (i.e., mean activation value of V1) across a large sequence of stimuli that varied only on a single dimension (i.e., variation due to stimulus change); 2) variability in activity across V1 neurons in response to a single stimulus (i.e., variation due to differential neuronal feature selectivity); and 3) fluctuation in the variability observed in case 2, across different levels of contrast. For practical reasons, we do not report on variability in response to a sequence of an unvarying stimulus because, due to characteristics of Topographica, even with biologically excessive modifications to models of V1 function, deviations from SDs of zero were uncommon and unreliable. On the other hand, reliable expansions or constrictions in firing rates were observed after selected manipulations when generating average responses

across V1 to a sequence of 1000 stimuli that systematically increased in contrast (i.e., case 1 above), when examining responses to neurons within a model V1 in response to a single stimulus (i.e., case 2 above), or when examining changes in variability within V1 across the same basic stimulus at different levels of contrast (i.e., case 3 above). Because response variability is often observed in psychiatric populations, including schizophrenia [10, 54], across trials that differ in stimulus characteristics, this approach is relevant to much published data and to clinical observations.

We also recognize that in many ways, a high level of variability in firing rates across neurons within a single region of cortex is desirable in that it can reflect reduced redundancy. In the models we tested, however, we aimed to determine whether the specific manipulations we introduced would be associated with variability levels that were greater than normal, with normal being defined as the amount of variability previously demonstrated in published studies using the GCAL model in which multiple aspects of normal visual functioning were successfully simulated [14, 21, 23-27]. We considered variability in excess of previously demonstrated normal levels to be pathological and to potentially be a cause of abnormal perception. This view is consistent with the ideas that precision in visual representation is the inverse of variability in sensory signals [55], and that excessive variability in brain activity in schizophrenia represents noise that is detrimental to efficient processing [56]. For example, activation of orientation-selective cells whose orientation preference is far from that of a visible stimulus would lead to both increased variability within the distribution of V1 cells, and to broadened orientation tuning, which could then impact processes that depend on precise representation of orientation, such as contour integration, motion discrimination, and facial emotion recognition, all of which are impaired in schizophrenia [3, 14]. It has also been demonstrated that both decreased and increased dopamine D1 receptor stimulation causes less distinctiveness in representations of stimulus patterns, due to a higher than normal number of neurons being active in coding many patterns [7]. Similarly, while some degree of neural noise can aid in detecting initially subthreshold signals by amplifying them so they can cross the detection threshold, an excess of noise can impair detection [6, 8].

The basic model development strategy was the same as in [14]. This involved: 1) developing a model of normal visual system function by training it with 10,000 pairs of stimuli (randomly-oriented Gaussians; see Figure 1); 2) making changes associated with a specific central nervous system (CNS) alteration (e.g., increased lateral excitation in V1; reduced retinal and LGN output, etc.) and running the model for another 10,000 iterations to allow for long-term adaptation to the new state; and 3) presenting new testing stimuli (sine wave gratings; see Figure 2) and measuring: a) average activation and variability across V1 neurons during a

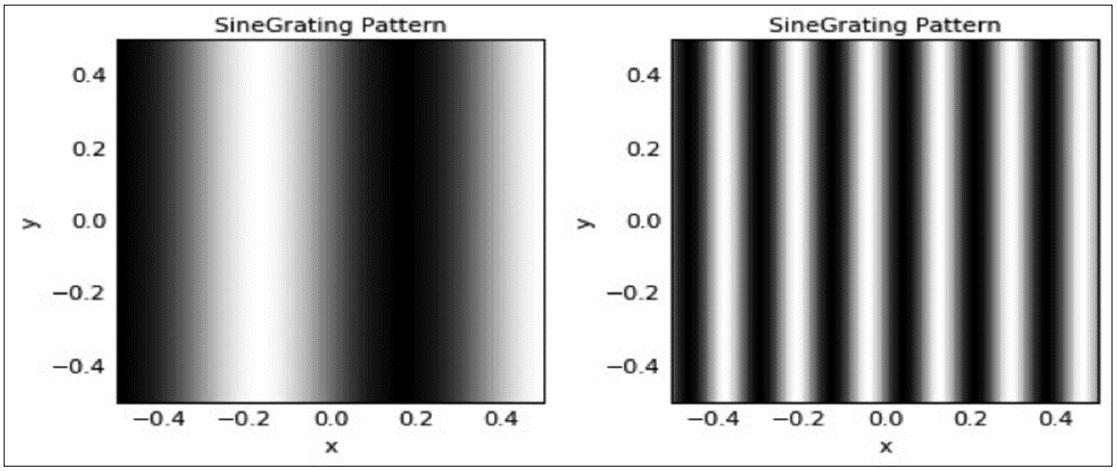

Figure 2. Stimuli used for post-training testing: Left – low spatial frequency stimulus (frequency = 1.5 cycles per image); Right – medium spatial frequency stimulus (frequency = 6 cycles per image).

sequence of 1000 stimuli, b) variability within V1 neurons in response to a single stimulus, or c) the fluctuation in variability within V1 neuron firing rates in response to a single stimulus as contrast is increased (in separate models). In addition, to examine variability after shorter-term CNS changes, we also developed a normal visual system model to 10,000, implemented CNS changes, and then immediately (i.e., without 10,000 additional trials) presented new stimuli and measured activation and variability in the same three scenarios described above.

Post-development testing stimuli consisted of low or medium spatial frequency (SF) sine wave gratings (see Figure 2). For measurement of variability within a stimulus sequence, we used sequences of 1000 trials for each sine-wave stimulus, in which the contrast on each presentation increased by 0.001, starting at 0.000 and ending at 0.999, with contrast defined as the proportion of the possible input range [23]. For each sequence of 1000 trials, data were collected on the mean and standard deviation (SD) of activity across all model V1 neurons. From these data, we calculated the relative standard deviation or coefficient of variation (CV) which is the standard deviation divided by the mean [57, 58]. We used the CV as our primary measure of neuronal variability because while the SD typically increases as the mean increases [and so, increased variability can be secondary to increased activation in general [e.g., as in [9, 13]], the CV expresses variability independent of the mean, and so it is scale invariant. The CV can also be thought of as reflecting the volatility of observed values around an expected value. This metric is commonly used to characterize stock market investments, where it provides investors with an estimate of the risk associated with a given investment over short-term intervals. For measurement of variability between different feature selective neurons in response to a single stimulus, the mean, SD, CV, and excess kurtosis values of activation levels across V1 sheet neurons in response to a single sine wave stimulus were generated. As with calculation of variability across stimulus transformations, CV was used as our primary measure of variability, with excess kurtosis used to represent excessive activation in orientation selective cells whose preference is far from that of the presented stimulus.

Hypotheses

Because increased excitatory activity can increase variability in neural network firing [56, 59], we expected that the greatest deviations from normal would arise from the manipulation that increased V1 activity to the greatest degree relative to unmodified models of V1 function. In our prior study this was a 15% reduction in retinal and LGN efferent activity, which led to a compensatory hyper-activation in V1 neurons. Because this effect was found mainly with low, but not medium SF stimuli, we expected to observe the same pattern here in terms of CV values. On the other hand, since impaired tuning is thought to be associated with increased variability as well, we expected that the model that best fit chronic schizophrenia data on reduced CS and broadened OR tuning in our past study (i.e., a 10% reduction in V1 lateral inhibition along with a threefold increase in the afferent learning rate at LGN-V1 connections [14]) would also be associated with an increased CV, in addition to an increase in excess kurtosis values, as previously observed.

Results

Overall, findings were similar for both LSF and MSF stimuli, but were more pronounced for LSF stimuli. Therefore, results for LSF stimuli only are described below.

Cross-stimuli Data (Variability Within a Stimulus Sequence)

Table 1, Row 1 demonstrates that when a normal V1 model is developed over 10,000 iterations, and then a CNS change is made, followed immediately by presentation of a sequence of 1000 stimuli with incrementally increasing contrast: 1) the highest level of activation (over double that observed in the unmodified model shown in Row 2, Column 1), and the largest SD are observed in the model with increased V1 lateral excitation; while 2) the weakest level of activation but the highest CV values are observed in the model with decreased retinal and LGN output. In contrast, Row 2 demonstrates that when a normal model is developed over 10,000 iterations, and then a CNS change is made followed by 10,000 additional development trials in the new CNS state, followed by presentation of the same 1000 trial stimulus sequence: 1) the models with either increased V1 lateral excitation or decreased V1 lateral inhibition generated the lowest levels of activation (owing to the development of compensatory inhibition)

Table 1. Activation and variability in models involving a 1000 trial run of the same LSF stimulus across 1000 levels of sequentially increasing contrast. Intra-cell structure is Mean | SD | CV.

Condition	Unmodified	10% ↑ V1 Lateral Excitation	10% ↓ V1 Lateral Inhibition	10% ↓ V1 Lateral Inhibition and 3x V1 Afferent Learning Rate	15% ↓ in Retinal and LGN Efferents
After initial 10,000 iterations	.018|.010|.556	.040|.024|.600	.024|.015|.625	.024|.015|.625	.002|.002|1.00
After a model change (except in next column) and then an additional 10,000 iterations	.019|.011|.579	.007|.005|.714	.010|.007|.700	.010|.007|.700	.028|.015|.536

Table 2. Activation and variability in models involving presentation of a single LSF test stimulus after model development. Intra-cell structure of each top line is Mean | SD | CV. Bottom value in each cell is excess kurtosis.

Condition	Unmodified	10% ↑ V1 Lateral Excitation	10% ↓ V1 Lateral Inhibition	10% ↓ V1 Lateral Inhibition and 3x V1 Afferent Learning Rate	15% ↓ in Retinal and LGN Efferents
After 10,000 iterations	.028|.064|2.28 9.49	.063|.155|2.46 12.07	.038|.086|2.26 9.00	.03|.086|2.26 9.00	.005|.019|3.80 32.18
After a model change (except in next column) and then an additional 10,000 iterations	.029|.068|2.34 11.39	.012|.046|3.83 44.45	.017|.053|3.12 22.55	.017|.050|2.94 27.87	.041|.081|1.97 7.43

but the largest CV value; and 2) the model with decreased retinal and LGN output generated the highest level of activation (owing to compensatory activity in V1, replicating Silverstein et al. (2017)), but the lowest CV value. Findings from these two models suggest that in the earliest phase of schizophrenia-related CNS dysregulation (which may begin in the prodromal phase), increased deviance from the normal range of excitation is likely to be related both to excess excitatory activity, as well as to variability that is independent of mean activity level (as reflected in CV values) that results from weakened input to V1. In contrast, with adaptation to these changes, a reversal occurs in which increased excitation is compensated for by increased lateral inhibition which lowers overall activation but leads to large increases in variability in V1 firing rates, while at the same time reduced input to V1 is compensated for by increased activation in V1 neurons but with reduced variability.

Single Trial Data (Variability Within V1)

Single trial data are presented in Table 2. Row 1 demonstrates that when a normal V1 model is developed over 10,000 iterations, and then a CNS change is made, followed immediately by presentation of a single test stimulus: 1) the highest level of activation (over double that observed in the unmodified model shown in Row 2, Column 2), and the largest SD are observed in the model with increased V1 lateral excitation; while 2) the weakest level of activation but the highest CV and excess kurtosis values are observed in the model with decreased retinal and LGN output. In contrast, Row 3 demonstrates that when a normal model is developed over 10,000 iterations, and then a CNS change is made followed by 10,000 additional development trials in the new CNS state, followed by presentation of a single test stimulus: 1) the models with increased V1 lateral excitation or reduced V1 lateral inhibition generated the lowest levels of activation (owing to the development of inhibition) but the largest CV and excess kurtosis values; and 2) the model with decreased retinal and LGN output generated the highest level of activation [owing to compensatory activity in V1], but the lowest CV and excess kurtosis values (see Figures 3 and 4). Taken together, and similar to the cross-stimuli data reported in the paragraph above, data from these two models suggest that in the earliest phase of acute schizophrenia-related CNS dysregulation, increased variability is likely to be related both to excess excitatory activity, as well as to variability that is independent of mean activity level (as reflected in CV values) that results from weakened input to V1. In contrast, with adaptation to these changes, a reversal occurs in which increased excitation is compensated for by increased lateral inhibition which lowers overall activation but leads to large increases in variability in V1 firing rates, while at the same time reduced input to V1 is compensated for by increased activation in V1 neurons but with reduced variability.

Variability of CV Across Different Levels of Contrast

Data on CV values across a range of contrast levels (each multiplied by a factor of 2) from 20% to 80% contrast are shown in Figure 5, for the case where the model was run normally for 10,000 trials, followed by a model change and then immediately by presentation of a single LSF test stimulus at one of the contrast levels. It can be seen here that manipulations involving increased excitation or reduced inhibition generally follow the normal pattern of change in variability across contrast level. In fact, the overlap is so great among most conditions and the unmodified condition that most data series are occluded in the graph. However, the clear deviant condition is the one with reduced retinal and LGN signaling. No data point is plotted for 20% contrast in this condition because the mean was 0 and so the CV could not be defined. However, at 40% contrast (where there is excessive noise relative to the weak signal) the CV is excessively high, and it remains higher than in all other conditions even at 80% contrast, as noted above.

For the case where the model was run normally for 10,000 trials, followed by a model perturbation and then 10,000 additional trials in which the effects of the manipulation were increasingly manifested, see Figure 6. Here, where the system has adapted to reduced sensory input: 1) variability is *lowest* across all contrast levels in the condition of reduced retinal and LGN output, and variability is highest in conditions with either increased excitation or reduced inhibition.

Discussion

The purpose of this study was to examine the effects of E/I imbalance, or factors hypothesized to be

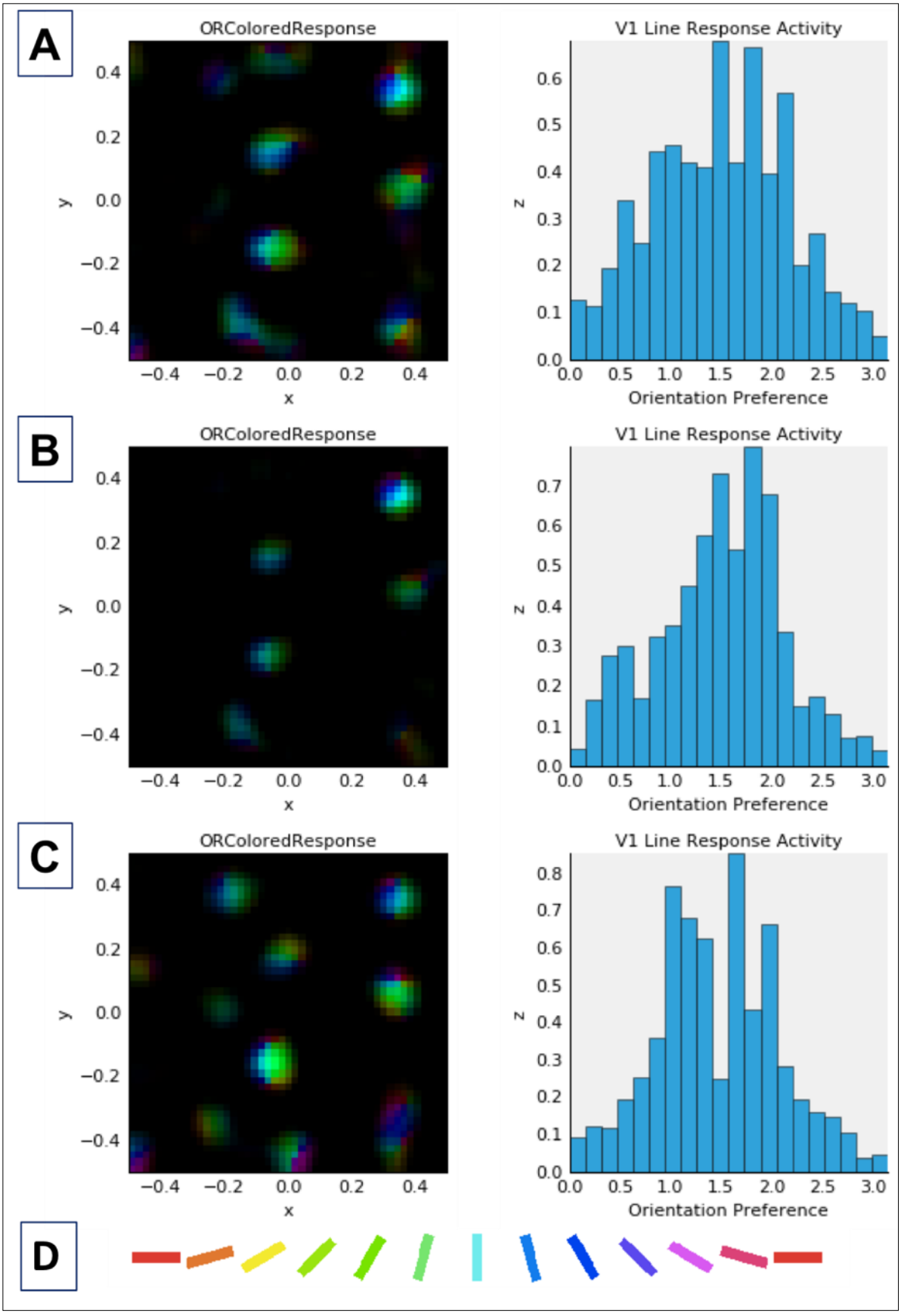
A
ORColoredResponse
V1 Line Response Activity
B
ORColoredResponse
V1 Line Response Activity
C
ORColoredResponse
V1 Line Response Activity
x
y
z
Orientation Preference
D

Figure 3. Combined activation and orientation preference maps (left column) and histograms showing activation of V1 neurons as a function of cell orientation preference (on x-axis, in radians) (right column). Data in both columns reflect activation in response to a single presentation of the LSF sine grating stimulus at 80% contrast (see Figure 2) after normal or abnormal model V1 development (see below). Each color in the maps in the left column corresponds to selectivity for the orientation denoted by the corresponding color in the key (D) at the bottom of this figure. Brightness corresponds to the firing rate of the neuron at a given location in the V1 sheet, which is retinotopic with respect to the LSF stimulus shown in Figure 2. In the histograms in the right column, the expected distribution peak for vertically oriented stimuli (see Figure 2) is $\pi/2$ or ~1.57 radians. A: Data for unmodified model after 20,000 iterations (same as in top row, Figure 4). B: Data after 10,000 normal development trials followed by 10,000 trials adapting to 10% increased V1 lateral excitation. This model is associated with the highest CV of all contrast ramp models (see Table 1). Note that the peak of the OR tuning histogram is not at the preferred orientation, which may account for some of the excess variability, in addition to the large drop from the peak to the tails, which is also asymmetrical. C: Data after 10,000 normal development trials, followed by implementation of 10% increased V1 lateral excitation, and then by immediate presentation of the 1000-stimulus sequence. Note the high level of excitation in this model (before generalized inhibition effects arise). This model demonstrates the highest mean activation of all contrast ramp models (note change in Y axis values relative to other models), and the highest SD, but not the highest CV or excess kurtosis. The latter can be observed both in the smaller tails in the histogram, as well as in the blue-green coloring in the activation map indicating that the excess activation was for orientation selective cells signaling vertical or near-vertical orientations. As with the model data in Row 2, the peak of the OR histogram is again not at preferred orientation, but is close to it (and activation in other model neurons is roughly symmetrical around it) with little activity at the tails, and less activity at the tails compared to the model after 20,000 developmental iterations. This increased drop in activation away from the peak can account for a portion of increased CV in this model.

related to it, on deviations from normal levels of variability in V1 firing rates in response to visual stimuli in computational models of visual system function in schizophrenia. Our main findings can be summarized as follows: 1) Reductions in signaling of sensory information, at the level of the retina and LGN, initially led to increases in variability of firing rates within the context of reduced V1 activation; but 2) with prolonged adaptation to weakened sensory signaling, compensatory hyper-activation in V1 neurons was observed, and variability was no longer increased over that observed in an unmodified V1; 3) in contrast to the effects of reduced sensory signaling, direct increases in the level of V1 lateral excitation led to the highest levels of initial activation but not the largest increase in firing rate variability, while 4) with prolonged adaptation to increased V1 lateral excitation or reduced V1 inhibition, overall activity was no longer higher than in the unmodified model due to compensatory inhibition, but a large increase in variability in firing rates was observed; 5) the patterns described above (in 1-4) were observed regardless of whether neural response variability was operationalized as differences between firing rates across V1 neurons in response to a single stimulus or differences between the overall firing rates within V1 across a set of 1000 stimuli that systematically increased in contrast by values of 0.001; 6) Paralleling these results, the fluctuation in variability (across V1 neurons) between 40% and 80% contrast levels in response to the same basic stimulus was largest in the condition of reduced sensory signaling when the stimulus was presented immediately after a manipulation to the model was made, but was lowest in this condition and highest in the condition of adaptation to increased V1 excitation when 10,000 trials were run after the manipulation but before presenting the test

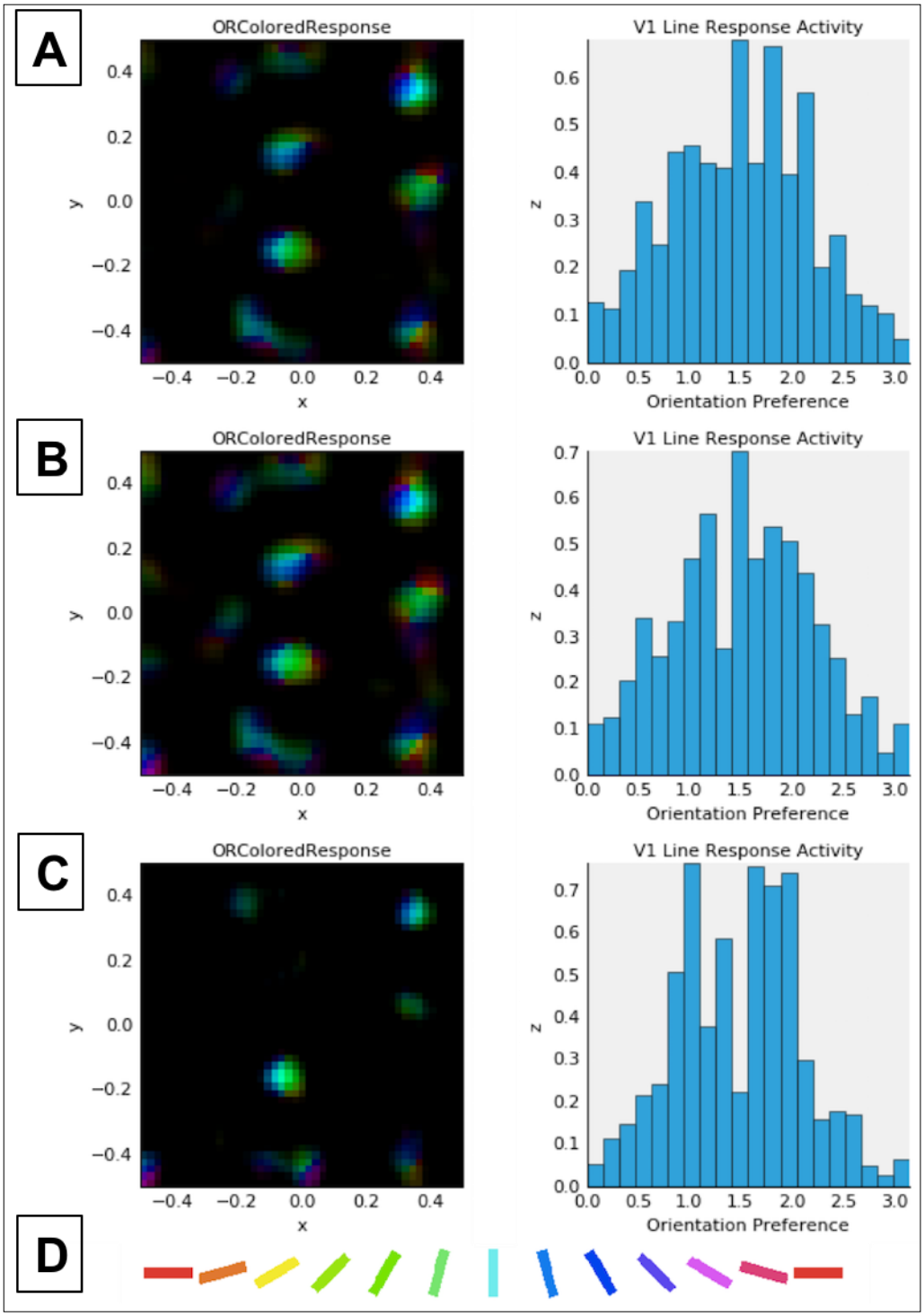

Figure 4. Combined activation and orientation preference maps (left column) and histograms showing activation of V1 neurons as a function of cell orientation preference (on x-axis, in radians) (right column). Data in both columns reflect activation in response to a single presentation of the LSF sine grating stimulus at 80% contrast (see Figure 2) after normal or abnormal model V1 development (see below). Each color in the maps in the left column corresponds to selectivity for the orientation denoted by the corresponding color in the key (D) at the bottom of this figure. Brightness corresponds to the firing rate of the neuron at a given location in the V1 sheet, which is retinotopic with respect to the LSF stimulus shown in Figure 2. In the histograms in the right column, the expected distribution peak for vertically oriented stimuli (see Figure 2) is $\pi/2$ or ~1.57 radians. A: Data for unmodified model after 20,000 iterations (same as in top row, Figure 3). B: Data after 10,000 normal development trials followed by 10,000 trials adapting to 15% reduced retinal and LGN output.

There is a higher level of activation here compared to the unmodified model, but variability is equivalent. C: Data after 10,000 normal development trials, followed by implementation of 15% reduced retinal and LGN output, and then by immediate presentation of the LSF stimulus without additional trials adapting to the CNS alteration. There is a lower level of activation here than in the other models involving a single stimulus test presentation, but a higher excess kurtosis value, and the highest CV of models tested using a single test stimulus (see Table 2), which is partly a function of the largest decrease in activation between the peaks and tails of the distribution. Data from this model also reveal the clearest example of broadened OR tuning in that there are multiple peaks, and compensatory inhibitory suppression of activity in cells that would normally be most responsive to the stimulus (i.e., at 1.57 radians). Data from an unmodified model at 10,001 iterations are not shown as results are virtually identical to the unmodified model at 20,001 (see Table 2).

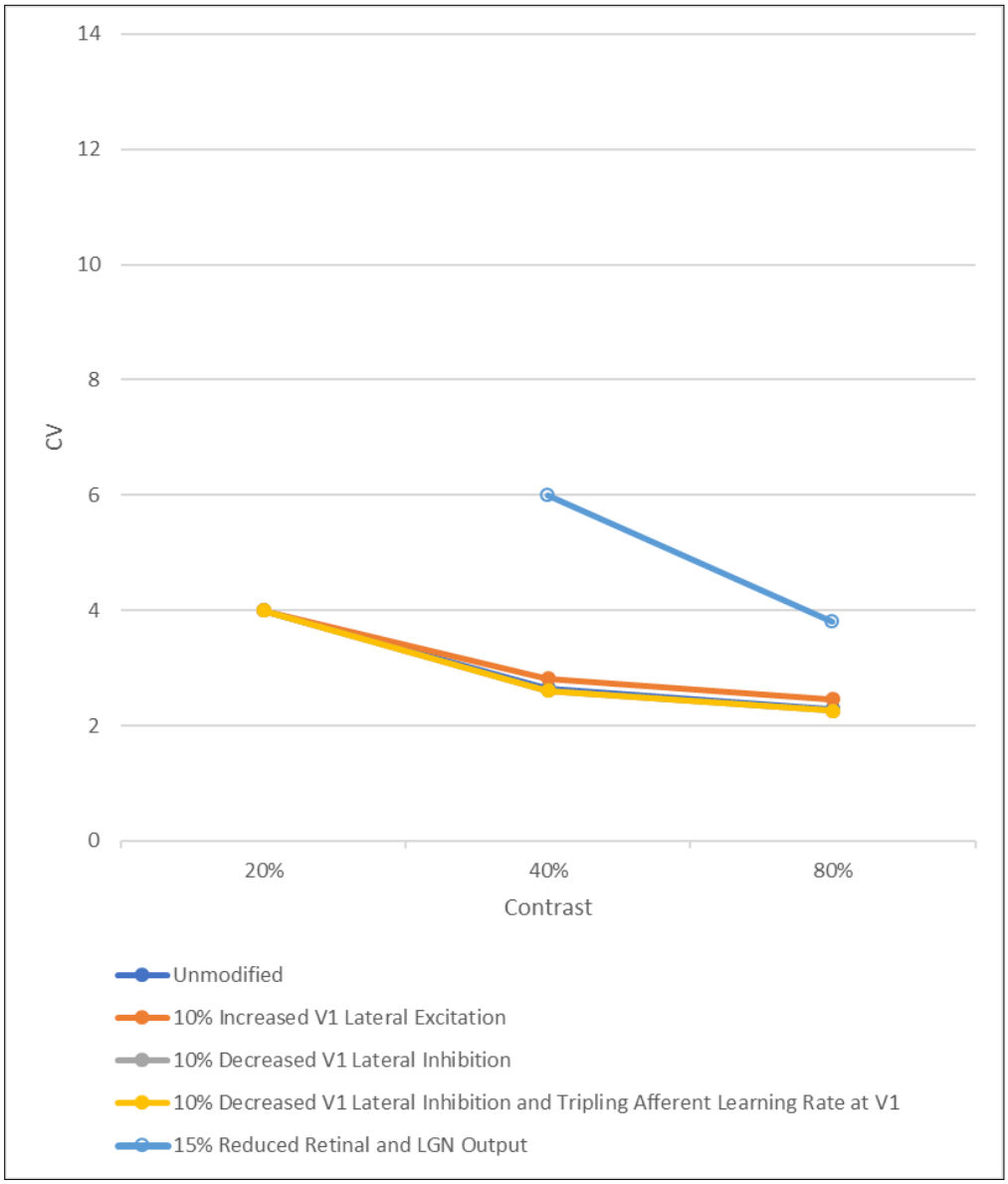

Figure 5. Coefficient of variation (CV) values in different contrast conditions, as a function of parameter manipulation type, after 10,000 trials of normal development followed by a model manipulation and then immediately by a presentation of an LSF sine-wave stimulus.

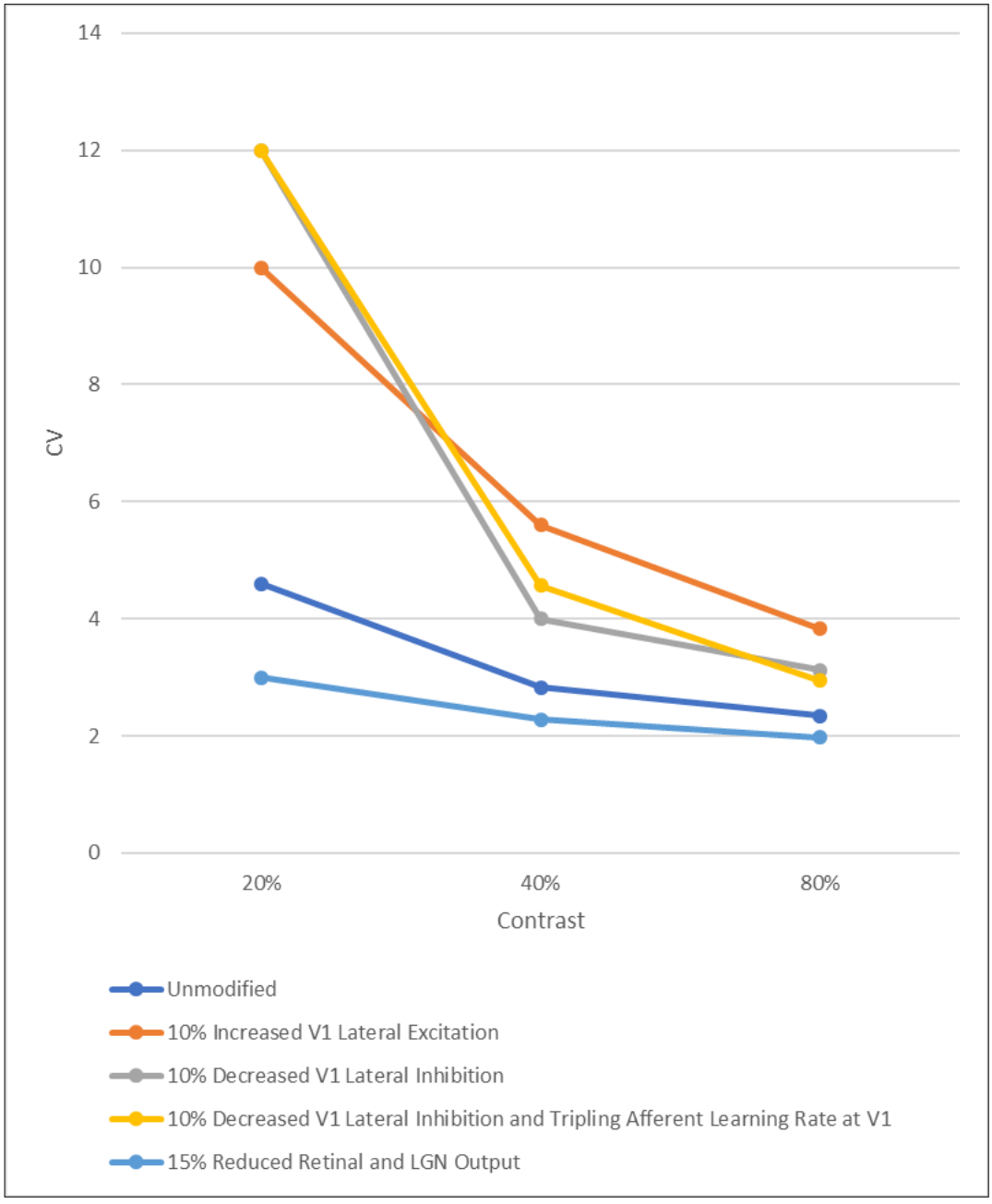

Figure 6. Coefficient of variation (CV) values in different contrast conditions, as a function of parameter manipulation type, after 10,000 trials of normal development followed by a model manipulation and then 10,000 additional trials and then presentation of an LSF sine-wave stimulus.

stimulus; and 7) when measuring firing rates across V1 neurons in response to a single stimulus, increased CV values were not a function of higher mean and SD values, but they were associated with increased excess kurtosis. This indicates that increased variability in neuronal firing rates is associated with increased activation in cells that normally do not respond as strongly to a specific stimulus, and therefore to reduced precision or broadened tuning.

While increased variability in firing rates was related to the lowest mean levels of activation in the models with direct and compensatory increases in excitation, it is important to note that higher CV values were not simply a function of lower mean values, and that CV and mean values are largely independent of each other, as can be seen in Tables 1 and 2. Given that CV values are not a function of either increases or decreases in mean activation values, they can be seen as representing an index of variability that is scale-invariant. We therefore recommend that future studies of schizophrenia and other psychiatric populations report on the CV in addition to reporting variability as a function of the standard deviation (as is typically done), since the latter may be strongly linked to overall level of activation. Another, related, advantage of the CV is that it can be used to directly compare variability across data sets, regardless of the phenomena being measured and their mean values.

One implication of the findings we report is that schizophrenia-related increases in firing rate variability (and therefore, in precision of stimulus processing) may arise from at least two causes: 1) a reduction in sensory input to cortex, prior to compensatory increases in excitation; and 2) inhibition secondary to increases in lateral excitation within V1 (which can also result from decreases in some forms of inhibition). The former is consistent with literature suggesting that some aspects of psychosis resemble effects of sensory deprivation [60, 61]. In support of this, reduced photoreceptor signaling (ERG a-wave amplitude) was associated with more severe positive symptoms in acutely ill schizophrenia patients [28]. This hypothesis is also consistent with the view that reduced sensory signaling represents a condition wherein signal-to-noise ratio is, by definition, low, and where there is subsequently an increase in intra-network random activation [7], leading to both less consistent identification of a single stimulus, and less precise discrimination between multiple stimuli (i.e., increased uncertainty). Such a situation, in which ineffective input to cortex was associated with increased noise and with increased neural variability in activity across stimulus conditions, has been observed in autism [11]. This view is also consistent with findings that increased variability is associated with flatter slopes in psychometric functions [62], and flatter psychometric functions have been observed many times in studies of perception in schizophrenia [15] [63-65]. The hypothesis that inhibition secondary to increases in lateral excitation within V1 is an additional cause of firing rate variability is consistent with NMDA receptor hypofunction leading to increased excitation [66, 67], and with evidence of increased baseline (i.e., pre-stimulus) gamma band [68] or beta-band [46] activity in schizophrenia. We further hypothesize that efforts to inhibit this state of excess excitation may result in an uneven or patchy pattern of E/I balance within an area of cortex (leading to increased variability in firing rates), especially if there are also impairments in GABA-ergic (inhibitory) signaling, which is another characteristic of schizophrenia [69-71]. All of these considerations suggest that increased firing rate variability, E/I imbalance, reduced neuronal tuning, and reduced signal-to-noise ratios may share, in part, common variance and origins in schizophrenia.

The phenomenology that we have simulated in this paper is consistent with current formulations of neuronal processing in schizophrenia based upon predictive coding. In brief, the current understanding is that precision or confidence assigned to sensory prediction errors is too high [72]. This induces a compensatory rebalancing of precision at higher levels in cortical hierarchies - to produce positive symptoms like hallucinations and delusions. Such a scenario fits comfortably with the above account on several levels. First, a failure to attenuate visual precision is, physiologically, exactly what we have modelled in terms of increases in excitation. In neuro-biologically plausible versions of predictive coding, precision is mediated through gain control mechanisms (probably involving inhibitory interneurons and fast synchronous oscillations) that modulate lateral interactions; here, within V1. Furthermore, our results show the importance of the

compensatory adaptation to this primary pathophysiology; here, in terms of plasticity and increased response variability. This precision-based account also lends the excitation-inhibition balance a functional interpretation; where the balance or cortical excitability plays the role of a (Kalman) gain control mechanism that weights sensory evidence to a greater or lesser degree during perceptual synthesis. Finally, the ensuing changes in the precision of representations in the visual cortex can be related to the precision (i.e. the spread) of the tuning curves that we have simulated. On the other hand, the precision of representations per se corresponds to the (negative) entropy in information theoretic treatments of visual processing.

There are several important limitations to this study. First, our critical metric, the CV, expressed deviation from the mean firing rate in our models, as opposed to deviation from a slope or curve at a given degree of a parameter manipulation. On the other hand, the same findings regarding variability occurred whether we defined variability as differences in overall V1 firing rates to a sequence of stimuli that changed along one dimension (contrast), differences in individual neuron firing rates within V1 in response to a single stimulus, or as fluctuation in variability in within-V1 firing rates to a single stimulus across levels of contrast. Therefore, our findings appear to be robust even though it is unknown at this point whether our conclusions would also apply in the case of deviation from a slope or curve. Moreover, a recent study in autism observed that an increase in level of variability across contrast levels was associated with reduced signal-to-noise ratio [11], which is consistent with our model findings regarding schizophrenia and reduced sensory signaling. Another limitation is that, due to characteristics of the Topographica modeling environment, we could not generate results for the case in which variability was measured in response to a single repeating (identical) stimulus. An additional limitation is that in humans, it is not currently possible to measure any of the types of variation in cell firing that we have discussed, and thus the application of our findings to people with schizophrenia remains in the realm of theoretical neurobiology. On the other hand, the findings generated in this study could be tested in animal models of schizophrenia using implanted electrodes. Of course, the major limitation of this study is that it used a computational model that, like all such models, is orders of magnitude simpler than the human brain, and so unable to capture a wide range of aspects of brain function. Finally, all GCAL models use feedforward and lateral connectivity only, whereas in the real brain there are backward or descending connections from V1 to LGN that we could not model. These are thought to play a predictive or contextualizing role and can have a profound effect on classical and extra-classical receptive field properties in V1. Having said that, the lateral interactions within our model can, mathematically, 'stand in' for recurrent effects.

In short, the computational modeling data presented here point to both reduced sensory signaling and adaptation to increased V1 lateral excitation (and to a lesser extent, reductions in V1 lateral inhibition) as contributors to increased neuronal firing rate variability in schizophrenia. Moreover, the two best fitting models also generated reduced precision in the form of broadened OR tuning, which can also be seen as a form of increased noise. And, even with the qualifications noted above, the two models that generated clear increases in firing rate variability suggest interesting directions for future work. One direction is continued exploration of the role of abnormal sensory processing in generating abnormal cortical activity, including psychotic symptoms. A second is further study of the developmental relationships between increases and decreases in cortical activation, increases in firing rate variability, reduced precision, signal-to-noise ratio, and behavioral function across phases and stages of illness.

Acknowledgments

The authors thank Michael Gara, Molly Erickson, Brian Keane, and Samantha Fradkin for their comments on an earlier draft of this paper.

Financial Disclosures

Steven Silverstein and Hristian Kourtev reported no biomedical financial interests or potential conflicts of interest. This project was not funded by any external funding source.

References

1. Heeger, D.J., M. Behrmann, and I. Dinstein, 2017 *Vision as a Beachhead.* DOI: 10.1016/ j.biopsych.2016.09.019. Biol Psychiatry. 81(10), 832-837.

2. Phillips, W.A. and S.M. Silverstein, 2003 *Convergence of biological and psychological perspectives on cognitive coordination in schizophrenia.* Behav Brain Sci. 26(1), 65-82; discussion 82-137.
3. Silverstein, S.M., 2016 *Visual Perception Disturbances in Schizophrenia: A Unified Model.* Nebr Symp Motiv. 63, 77-132.
4. Silverstein, S.M. and B.P. Keane, 2011 *Vision Science and Schizophrenia Research: Toward a Re-view of the Disorder Editors' Introduction to Special Section.* DOI: sbr053 [pii]10.1093/schbul/sbr053. Schizophr Bull. 37(4), 681-9.
5. Silverstein, S.M. and J.L. Thompson, 2015 *A vision science perspective on schizophrenia.* DOI: 10.1016/j.scog.2015.05.003. Schizophr Res Cogn. 2(2), 39-41.
6. Li, S., T. von Oertzen, and U. Lindenberger, 2006 *A neurocomputational model of stochastic resonance and aging.* Neurocomputing. 69, 1553–1560.
7. Li, S.C. and S. Sikstrom, 2002 *Integrative neurocomputational perspectives on cognitive aging, neuromodulation, and representation.* Neurosci Biobehav Rev. 26(7), 795-808.
8. MacDonald, S.W., S.C. Li, and L. Backman, 2009 *Neural underpinnings of within-person variability in cognitive functioning.* DOI: 10.1037/a0017798. Psychol Aging. 24(4), 792-808.
9. Northoff, G., et al., 2018 *Too Fast or Too Slow? Time and Neuronal Variability in Bipolar Disorder-A Combined Theoretical and Empirical Investigation.* DOI: 10.1093/schbul/sbx050. Schizophr Bull. 44(1), 54-64.
10. Russell, V.A., et al., 2006 *Response variability in Attention-Deficit/Hyperactivity Disorder: a neuronal and glial energetics hypothesis.* DOI: 10.1186/1744-9081-2-30. Behav Brain Funct. 2, 30.
11. Weinger, P.M., et al., 2014 *Low-contrast response deficits and increased neural noise in children with autism spectrum disorder.* DOI: 10.1016/j.neuropsychologia.2014.07.031. Neuropsychologia. 63, 10-18.
12. Rentrop, M., et al., 2010 *Intra-individual variability in high-functioning patients with schizophrenia.* DOI: 10.1016/j.psychres.2010.04.009. Psychiatry Res. 178(1), 27-32.
13. Shin, K.S., et al., 2015 *Intraindividual neurophysiological variability in ultra-high-risk for psychosis and schizophrenia patients: single-trial analysis.* DOI: 10.1038/npjschz.2015.31. NPJ Schizophr. 1, 15031.
14. Silverstein, S.M., D. Demmin, and J.A. Bednar, 2017 *Computational modeling of contrast sensitivity and orientation tuning in first-episode and chronic schizophrenia.* Computational Psychiatry. 1, 102-131.
15. Butler, P.D., S.M. Silverstein, and S.C. Dakin, 2008 *Visual perception and its impairment in schizophrenia.* DOI: 10.1016/j.biopsych.2008.03.023. Biol Psychiatry. 64(1), 40-7.
16. Silverstein, S.M. and R. Rosen, 2015 *Schizophrenia and the eye.* Schizophrenia Research: Cognition. 2 (2), 46-55.
17. Gao, R. and P. Penzes, 2015 *Common mechanisms of excitatory and inhibitory imbalance in schizophrenia and autism spectrum disorders.* Curr Mol Med. 15(2), 146-67.
18. Starc, M., et al., 2017 *Schizophrenia is associated with a pattern of spatial working memory deficits consistent with cortical disinhibition.* DOI: 10.1016/j.schres.2016.10.011. Schizophr Res. 181, 107-116.
19. Krystal, J.H., et al., 2017 *Impaired Tuning of Neural Ensembles and the Pathophysiology of Schizophrenia: A Translational and Computational Neuroscience Perspective.* DOI: 10.1016/j.biopsych.2017.01.004. Biol Psychiatry. 81(10), 874-885.
20. Bednar, J.A., 2009 *Topographica: Building and Analyzing Map-Level Simulations from Python, C/C++, MATLAB, NEST, or NEURON Components.* DOI: 10.3389/neuro.11.008.2009. Front Neuroinform. 3, 8.
21. Bednar, J.A., 2012 *Building a mechanistic model of the development and function of the primary visual cortex.* DOI: 10.1016/j.jphysparis.2011.12.001. J Physiol Paris. 106(5-6), 194-211.
22. Bednar, J.A., A. Kelkar, and R. Miikkulainen, 2004 *Scaling self-organizing maps to model large cortical*

networks. DOI: 10.1385/NI:2:3:275. Neuroinformatics. 2(3), 275-302.

23. Stevens, J.L., et al., 2013 *Mechanisms for stable, robust, and adaptive development of orientation maps in the primary visual cortex.* DOI: 10.1523/JNEUROSCI.1037-13.2013. J Neurosci. 33(40), 15747-66.
24. Bednar, J.A., *Hebbian learning of the statistical and geometrical structure of visual input*, in *Neuromathematics of vision*, Citti G. and S. A., Editors. 2014, Springer: New York. p. 335-366.
25. Bednar, J.A., *Constructing complex systems via activity-driven unsupervised Hebbian self-organization*, in *Growing adaptive machines*, T. Kowaliw, N. Bredeche, and R. Doursat, Editors. 2014, Springer: New York. p. 201-225.
26. Bednar, J.A. and S.P. Wilson, 2016 *Cortical Maps.* DOI: 10.1177/1073858415597645. Neuroscientist. 22(6), 604-617.
27. Miikkulainen, R., et al., 2005 *Computational maps in the visual cortex*. 2005, New York, NY: Springer.
28. Balogh, Z., G. Benedek, and S. Keri, 2008 *Retinal dysfunctions in schizophrenia.* DOI: 10.1016/j.pnpbp.2007.08.024. Prog Neuropsychopharmacol Biol Psychiatry. 32(1), 297-300.
29. Demmin, D.L., et al., 2018 *Electroretinographic anomalies in schizophrenia.* DOI: 10.1037/abn0000347. J Abnorm Psychol. 127(4), 417-428.
30. Hébert, M., et al., 2010 *Retinal response to light in young nonaffected offspring at high genetic risk of neuropsychiatric brain disorders.* DOI: 10.1016/j.biopsych.2009.08.016. Biol Psychiatry. 67(3), 270-4.
31. Hébert, M., et al., 2015 *Light evoked potentials measured by electroretinogram may tap into the neurodevelopmental roots of schizophrenia.* DOI: 10.1016/j.schres.2014.12.030. Schizophr Res. 162(1-3), 294-5.
32. Lavoie, J., et al., 2014 *The electroretinogram as a biomarker of central dopamine and serotonin: potential relevance to psychiatric disorders.* DOI: 10.1016/j.biopsych.2012.11.024. Biol Psychiatry. 75 (6), 479-86.
33. Lavoie, J., M. Maziade, and M. Hebert, 2014 *The brain through the retina: the flash electroretinogram as a tool to investigate psychiatric disorders.* DOI: 10.1016/j.pnpbp.2013.09.020. Prog Neuropsychopharmacol Biol Psychiatry. 48, 129-34.
34. Shagass, C. and R. Roemer, 1991 *Evoked potential topography in unmedicated and medicated schizophrenics.* Int J Psychophysiol. 10(3), 213-24.
35. Shagass, C., J.J. Straumanis, and R.A. Roemer, 1982 *Psychotropic drugs and evoked potentials.* Electroencephalogr Clin Neurophysiol Suppl. 36, 538-48.
36. Straumanis, J.J., C. Shagass, and R.A. Roemer, 1982 *Influence of antipsychotic and antidepressant drugs on evoked potential correlates of psychosis.* Biol Psychiatry. 17(10), 1101-22.
37. Yoon, J.H., et al., 2010 *GABA concentration is reduced in visual cortex in schizophrenia and correlates with orientation-specific surround suppression.* DOI: 10.1523/JNEUROSCI.6158-09.201030/10/3777 [pii]. J Neurosci. 30(10), 3777-81.
38. Kelemen, O., et al., 2013 *Perceptual and cognitive effects of antipsychotics in first-episode schizophrenia: the potential impact of GABA concentration in the visual cortex.* DOI: 10.1016/j.pnpbp.2013.07.024. Prog Neuropsychopharmacol Biol Psychiatry. 47, 13-19.
39. Thakkar, K.N., et al., 2017 *7T Proton Magnetic Resonance Spectroscopy of Gamma-Aminobutyric Acid, Glutamate, and Glutamine Reveals Altered Concentrations in Patients With Schizophrenia and Healthy Siblings.* DOI: 10.1016/j.biopsych.2016.04.007. Biol Psychiatry. 81(6), 525-535.
40. Katzner, S., L. Busse, and M. Carandini, 2011 *GABAA inhibition controls response gain in visual cortex.* DOI: 10.1523/JNEUROSCI.5753-10.2011. J Neurosci. 31(16), 5931-41.
41. Anticevic, A., et al., 2013 *Connectivity, pharmacology, and computation: toward a mechanistic understanding of neural system dysfunction in schizophrenia.* DOI: 10.3389/fpsyt.2013.00169. Front Psychiatry. 4, 169.

42. Anticevic, A., et al., 2015 *N-methyl-D-aspartate receptor antagonist effects on prefrontal cortical connectivity better model early than chronic schizophrenia.* DOI: 10.1016/j.biopsych.2014.07.022. Biol Psychiatry. 77(6), 569-80.

43. Corlett, P.R., et al., 2011 *Glutamatergic model psychoses: prediction error, learning, and inference.* DOI:10.1038/npp.2010.163. Neuropsychopharmacology. 36(1), 294-315.

44. Silverstein, S.M., et al., 2012 *Absolute level of gamma synchrony is increased in first-episode schizophrenia during face processing.* Journal of Experimental Psychopathology. 3(4), 702-723.

45. Rivolta, D., et al., 2014 *Source-reconstruction of event-related fields reveals hyperfunction and hypofunction of cortical circuits in antipsychotic-naive, first-episode schizophrenia patients during Mooney face processing.* DOI: 10.1523/JNEUROSCI.3752-13.2014. J Neurosci. 34 (17), 5909-17.

46. Sun, L., et al., 2013 *Evidence for dysregulated high-frequency oscillations during sensory processing in medication-naive, first episode schizophrenia.* DOI: 10.1016/j.schres.2013.08.023. Schizophr Res. 150(2-3), 519-25.

47. Hamm, J.P., et al., 2017 *Altered Cortical Ensembles in Mouse Models of Schizophrenia.* DOI: 10.1016/j.neuron.2017.03.019. Neuron. 94(1), 153-167 e8.

48. Anticevic, A., et al., 2014 *Characterizing thalamo-cortical disturbances in schizophrenia and bipolar illness.* DOI: 10.1093/cercor/bht165. Cereb Cortex. 24(12), 3116-30.

49. DeAngelis, G.C., R.D. Freeman, and I. Ohzawa, 1994 *Length and width tuning of neurons in the cat's primary visual cortex.* J Neurophysiol. 71(1), 347-74.

50. Sceniak, M.P., M.J. Hawken, and R. Shapley, 2001 *Visual spatial characterization of macaque V1 neurons.* J Neurophysiol. 85(5), 1873-87.

51. Rochester, N., et al., 1956 *Tests on a cell assembly theory of the action of the brain, using a large digital computer.* IRE Transactions on Information Theory. 2, 80-93.

52. Carandini, M. and D.J. Heeger, 2011 *Normalization as a canonical neural computation.* DOI: 10.1038/nrn3136. Nat Rev Neurosci. 13(1), 51-62.

53. Coen-Cagli, R. and O. Schwartz, 2013 *The impact on midlevel vision of statistically optimal divisive normalization in V1.* DOI: 10.1167/13.8.13. J Vis. 13, 8.

54. Cole, V.T., D.R. Weinberger, and D. Dickinson, 2011 *Intra-individual variability across neuropsychological tasks in schizophrenia: a comparison of patients, their siblings, and healthy controls.* DOI: 10.1016/j.schres.2011.03.007. Schizophr Res. 129(1), 91-3.

55. Brown, H.R. and K.J. Friston, 2012 *Dynamic causal modelling of precision and synaptic gain in visual perception - an EEG study.* DOI: 10.1016/j.neuroimage.2012.06.044 S1053-8119(12)00659-3 [pii]. Neuroimage. 63(1), 223-31.

56. Rolls, E.T., et al., 2008 *Computational models of schizophrenia and dopamine modulation in the prefrontal cortex.* DOI: 10.1038/nrn2462. Nat Rev Neurosci. 9(9), 696-709.

57. Reed, G.F., F. Lynn, and B.D. Meade, 2002 *Use of coefficient of variation in assessing variability of quantitative assays.* Clin Diagn Lab Immunol. 9(6), 1235-9.

58. Forkman, J., 2009 *Estimator and tests for common coefficients of variation in normal distributions.* Communications in Statistics - Theory and Methods. 38(2), 233-251.

59. Rolls, E.T. and G. Deco, 2011 *A computational neuroscience approach to schizophrenia and its onset.* DOI: 10.1016/j.neubiorev.2010.09.001. Neurosci Biobehav Rev. 35(8), 1644-53.

60. Rosenzweig, N., 1959 *Sensory deprivation and schizophrenia: some clinical and theoretical similarities.* DOI: 10.1176/ajp.116.4.326. Am J Psychiatry. 116, 326-9.

61. Corlett, P.R., C.D. Frith, and P.C. Fletcher, 2009 *From drugs to deprivation: a Bayesian framework for understanding models of psychosis.* DOI: 10.1007/s00213-009-1561-0. Psychopharmacology (Berl). 206(4), 515-30.

62. Parker, A.J. and W.T. Newsome, 1998 *Sense and the single neuron: probing the physiology of*

perception. DOI: 10.1146/annurev.neuro.21.1.227. Annu Rev Neurosci. 21, 227-77.

63. Li, C.S., 2002 *Impaired detection of visual motion in schizophrenia patients.* Prog Neuropsychopharmacol Biol Psychiatry. 26(5), 929-34.
64. Li, C.S., et al., 2002 *Altered performance of schizophrenia patients in an auditory detection and discrimination task: exploring the 'self-monitoring' model of hallucination.* Schizophr Res. 55(1-2), 115-28.
65. Silverstein, S.M., et al., 2009 *An fMRI examination of visual integration in schizophrenia.* DOI: S0219635209002113 [pii]. J Integr Neurosci. 8(2), 175-202.
66. Krystal, J.H., et al., 2003 *NMDA receptor antagonist effects, cortical glutamatergic function, and schizophrenia: toward a paradigm shift in medication development.* DOI: 10.1007/s00213-003-1582-z. Psychopharmacology (Berl). 169(3-4), 215-33.
67. Moghaddam, B. and D. Javitt, 2012 *From revolution to evolution: the glutamate hypothesis of schizophrenia and its implication for treatment.* DOI: 10.1038/npp.2011.181. Neuropsychopharmacology. 37(1), 4-15.
68. Silverstein, S.M., et al., 2012 *Absolute level of gamma synchrony is increased in first episode schizophrenia during face processing.* Journal of Experimental Psychopathology. 3, 702-723.
69. Gonzalez-Burgos, G., R.Y. Cho, and D.A. Lewis, 2015 *Alterations in Cortical Network Oscillations and Parvalbumin Neurons in Schizophrenia.* DOI: 10.1016/j.biopsych.2015.03.010. Biol Psychiatry. 77 (12), 1031-1040.
70. Gonzalez-Burgos, G., K.N. Fish, and D.A. Lewis, 2011 *GABA neuron alterations, cortical circuit dysfunction and cognitive deficits in schizophrenia.* DOI: 10.1155/2011/723184. Neural Plast. 2011, 723184.
71. Phillips, W.A., A. Clark, and S.M. Silverstein, 2015 *On the functions, mechanisms, and malfunctions of intracortical contextual modulation.* DOI: 10.1016/j.neubiorev.2015.02.010. Neurosci Biobehav Rev. 52, 1-20.
72. Corlett, P.R., G.D. Honey, and P.C. Fletcher, 2016 *Prediction error, ketamine and psychosis: An updated model.* DOI: 10.1177/0269881116650087. J Psychopharmacol. 30(11), 1145-1155.